JNEST EISSN: 2961-8738 ● PISSN: 2961-8916 ● DOI: 10.56741/jnest.v4i03.1272
Article Received 19 July 2025, Revised 17 September 2025

Multimodal Gait Analysis Using IMU and EMG Sensors with HMM Classification to Differentiate Obese and Normal Body Types

Suto Setiyadi*, Muhammad Ridho Rosa, Nigel Bryan Tang, Muhammad Sabiq Al Muttaqin, Muhammad Rafi Haykal Gumelar

***Abstract*— Gait analysis is essential for diagnosing movement disorders and monitoring rehabilitation progress; conventional methods are often costly and complex. This study aims to differentiate gait characteristics between individuals with obesity and those with normal body composition using a multimodal approach that integrates Inertial Measurement Unit (IMU) and electromyography (EMG) sensors. Ten male participants (five obese, five normal) performed slow and fast walking trials with IMU sensor placement and EMG recording. Acceleration, gyroscope, and EMG data were analyzed using statistical tests (T-test and Mann–Whitney U) and 8-state HMM Model for gait sub-phase classification. On average, obese participants completed 129.8 steps in 84.2 s (slow) and 117.2 steps in 63.8 s (fast), compared to normal-weight participants with 127.4 steps in 77.6 s and 113.2 steps in 59.8 s. Significant differences ($p < 0.00001$) were found in acceleration (ax, ay) and EMG activity of the gastrocnemius and tibialis anterior. Gyroscope variance was higher in the obese group (e.g., state 0: 471.8 vs 249.6), indicating greater movement fluctuations. HMM distributions revealed a dominance of a single state among obese participants (e.g., gastrocnemius state 1: 54.3%; tibialis anterior state 1: 58.1%), whereas normal-weight participants showed more balanced distributions. Model evaluation identified the accelerometer as the most informative sensor (log-likelihood: obese slow walking 147,158.66 vs normal 39,928.33). Overall, the findings suggest that obese participants tend to exhibit slower, less efficient, and more variable gait patterns, while normal-weight participants display relatively more rhythmic and stable steps. Multimodal sensor integration with HMM provided promising results in distinguishing gait patterns between groups and may be further developed to support applications in rehabilitation and clinical assessment.**

***Index Terms*—Gait Analysis, Electromyography (EMG), Inertial Measurement Unit (IMU), Obese, Hidden Markov Model (HMM), Wearable Sensor**

I. INTRODUCTION

GAIT analysis plays a vital role in clinical diagnostics, rehabilitation, and biomechanical research by offering insights into musculoskeletal function and locomotor abnormalities [1], [2]. Traditional gait analysis methods, such as optical motion capture and force plates, provide high accuracy but are limited by high costs, stationary laboratory settings, and operational complexity [3]. Recent advances in wearable technology—particularly inertial measurement units (IMUs) and surface electromyography (EMG)—have enabled real-time, non-invasive, and portable gait assessments, making them more suitable for broader clinical and field applications [4], [5].

Obesity, defined as a body mass index (BMI) of ≥30 kg/m² [6], significantly alters gait biomechanics due to increased body mass, joint loading, and compensatory neuromuscular strategies [7]. Moreover, individuals with obesity exhibit a consistent mechanical influence on gait kinematics and strategies even among young adults where such alterations persist in the absence of pain or injury, indicating distinct biomechanical adaptations that cannot be fully explained by pathological factors alone [8], [9]. Obese participants generally demonstrate shorter step length, slower walking speed, wider step width, and longer double support time compared to individuals with normal body weight [10], [11]. IMU sensors have been effectively utilised to quantify these kinematic alterations [12], while EMG sensors provide complementary information by capturing the underlying muscle activation patterns [13]. However, most existing studies analyse these modalities in isolation, lacking a comprehensive integration of kinematic and neuromuscular data.

To address this gap, the present study proposes a multimodal gait analysis framework that integrates IMU and EMG sensors to differentiate gait characteristics between participants with obese and normal body types. The IMU sensors capture spatiotemporal parameters such as acceleration, gyroscope, and step duration [11], whereas EMG sensors monitor muscle activity in key lower limb muscles, namely the tibialis anterior and gastrocnemius [14]. Data acquisition is implemented using Bluetooth Low Energy (BLE)-enabled ESP32 microcontrollers for wireless and real-time monitoring. The main contributions of this study are as follows:

1. Multimodal Sensor Integration: Simultaneous acquisition of kinematic and neuromuscular signals to provide a comprehensive understanding of gait mechanics in both obese and normal individuals.
2. Robust Pattern Recognition: Implementation of a Hidden Markov Model (HMM) to classify gait phases during both fast and slow walking in obese and normal subjects.

This framework was validated on ten adult male participants (five with obesity and five with normal body weight), demonstrating its potential for objective gait evaluation and its relevance to personalised rehabilitation strategies for obesity-related movement disorders. Additionally, this study examined differences in gait

Suto Setiyadi, **Muhammad Ridho Rosa**, **Nigel Bryan Tang**, **Muhammad Sabiq Almuttaqin**, and **Muhammad Rafi Haykal Gumelar** are with the Department of Electrical Engineering, Telkom University, Indonesia.
*Correspondence: sutosetiyadisod@telkomuniversity.ac.id.

patterns between obese and non-obese participants, without considering the influence of other variables.

II. RESEARCH METHODOLOGY

This study uses a quantitative method to analyze gait characteristics in participants with normal and obese body types using a multimodal sensor system. The method has two main parts: collecting data and processing data. Data processing includes four steps: pre-processing, selecting features, analyzing with a HMM, and visualizing the data. The HMM model uses eight different states as shown in Fig. 2. The eight-state HMM used in this study reflects typical biomechanical subphases in gait rather than a strict one-to-one mapping with each cycle. The multiplication by eight was used to approximate the expected length of the state sequence during initialization.

A. Data Processing

Data processing is an essential step in research, aimed at converting raw data into useful information through structured procedures. Its main goals are to improve data quality, extract relevant information, and prepare the data for further analysis or modelling [15]. This study's data processing consists of three main stages: pre-processing, feature selection, and data analysis using statistical methods (t-test and Mann–Whitney U) and the HMM.

Pre-processing is conducted to correct or remove errors, inconsistencies, and missing values in the dataset. This step ensures clean and reliable data for analysis and modelling [16]. The EMG data from each obese and non-obese participant were combined, and the Root Mean Square (RMS) value was calculated for each walking condition (fast or slow) for each feature. The RMS formula is presented in (1). These parameters were selected to capture signal energy and deviation in gait signals. The magnitude was employed as the extracted feature for acceleration and gyroscope signals, as presented in (2).

$$\mathrm{RMS} = \sqrt{\frac{1}{\mathrm{n}}\sum_{\mathrm{i}=0}^{\mathrm{n}} \mathrm{x}_{\mathrm{i}}^2} \tag{1}$$

$$\mathrm{A_{mag}} = \sqrt{\mathrm{a_x^2} + \mathrm{a_y^2} + \mathrm{a_z^2}} \tag{2}$$

where μ denotes the mean, x_i represents the i-th data point, and N is the total number of data points. RE denotes the relative error, where x refers to the measured value and x_{ref} represents the reference or true value. RMS stands for Root Mean Square, and n indicates the total number of data samples. A_{mag} denotes the total acceleration magnitude, and a_x, a_y, a_z are the respective accelerations on each axis and for the gyroscope magnitude, it was replaced with g_x, g_y, dan g_z [17].

Feature selection focuses on identifying the most relevant features to enhance model accuracy and efficiency [18]. In the analysis of IMU and EMG data, filter-based feature selection methods are commonly employed, as they evaluate the relevance of each feature based on correlation metrics or independent statistical properties before modelling. In this study, filter-based methods are used for IMU and EMG data, selecting features based on statistical relevance before modelling [19].

Butterworth filter to reduce noise while maintaining key signal characteristics. This filter is chosen for its smooth frequency response and effectiveness in eliminating unwanted frequencies in EMG signals (20–500 Hz) and IMU data (cutoff ~10 Hz) [18], [20].

1) Statistical analysis

Statistical analysis was performed to compare acceleration, gyroscope, and EMG data between obese and non-obese groups. For variables meeting the assumptions of normality and homogeneity of variance, an independent samples t-test was applied. The non-parametric Mann–Whitney U test was used when these assumptions were violated. These tests aimed to identify significant differences in gait-related biomechanical parameters between the two groups [21]. The formulas for calculating the T-test and Mann–Whitney U are presented in (3) and (5).

$$\mathrm{t} = \frac{\bar{X}_1 - \bar{X}_2}{\sqrt{s_p^2\left(\frac{1}{n_1}+\frac{1}{n_2}\right)}} \tag{3}$$

$$s_p^2 = \frac{(n_1-1)s_1^2 + (n_2-1)s_2^2}{n_1+n_2-2} \tag{4}$$

where t is calculated by taking the difference between the sample means, divided by the standard error of the difference, s_p^2 is computed as a weighted average of the variances from both groups, accounting for their respective sample sizes, $\bar{X}$ represents the sample means of groups, s_1^2 & s_2^2 denotes the sample variances of groups, and n_1 & n_2 indicates the sample sizes of groups.

$$U = \min(U_1, U_2) \tag{5}$$

$$U_1 = n_1 n_2 + \frac{n_1(n_1+1)}{2} - R_1 \tag{6}$$

$$U_2 = n_1 n_2 + \frac{n_2(n_2+1)}{2} - R_2 \tag{7}$$

where n_1 & n_2 represent the sample sizes of groups 1 and 2, respectively, while R_1 & R_2 denote the sum of ranks for groups 1 and 2 after all data have been combined and ranked.

2) Hidden Markov Model

The HMM is a statistical framework for modelling stochastic processes characterised by a sequence of hidden (latent) states, where only the observable outputs generated by these states are accessible for analysis [22], [23]. HMMs are widely utilised in gait phase detection based on IMU data, as well as in the analysis of EMG signals for human motion recognition [24]. In the context of gait phase detection, implementing the model commonly involves using the transition matrix (A), the emission distribution (B), and the initial state probability vector. The HMM formulation (λ) for gait phase detection is presented in (8) through (11). In these equations, q_t is denotes the state of the system at time t, s_j is represents a specific state within the set of all possible states $\mathrm{S} = \{\mathrm{s1}, \mathrm{s2}, \ldots, \mathrm{sN}\}$, $b_j(o_t)$ is the probability that state s_j generates observation o_t and π_i is denotes the probability that the system is in state s_i at time t=1 [24].

$$A = [a_{ij}],\ a_{ij} = P(q_{t+1} = s_j | q_t = s_i) \tag{8}$$

$$B = [b_j], b_j(o_t) = P(o_t|q_t = s_j) \quad (9)$$

$$\pi = \{\pi_i\}, \pi_i = P(q_1 = s_i) \quad (10)$$

$$\lambda = (A, B, \pi) \quad (11)$$

In the HMM model, the observation sequence consists of concatenated IMU (accelerometer and gyroscope) and EMG features. Emission probabilities $b_j(o_t)$ were modeled using single-component Gaussian distributions with parameters estimated from training data for each hidden state. Transition probabilities a_{ij} and initial state π_i probabilities were optimized using the Baum–Welch algorithm during unsupervised training. The evaluation of the Hidden Markov Model (HMM) in this study uses three metrics: Log-Likelihood (LL), Akaike Information Criterion (AIC), and Bayesian Information Criterion (BIC). Log-likelihood measures how well the model fits the data, but using it alone can cause overfitting, especially in models with many parameters. To overcome this, AIC balances model fit and complexity, while BIC applies a stronger penalty for complexity, making it more effective for selecting the optimal number of states [25].

B. *Data Acquisition*

Data acquisition refers to capturing and converting signals from physical phenomena into digital data using sensors for computerised analysis [26]. This research involved procedures with negligible risk. Participants were instructed to wear leg-mounted sensors secured with a textile adapter and to walk a few steps for data collection. No invasive or semi-invasive activities were carried out. Before participation, all individuals received a written informed consent form that explained the study process, confirmed the absence of any risks beyond those associated with ordinary walking, and outlined their right to withdraw at any point without penalty. Only those who voluntarily signed the consent form were included in the study. Participants were limited to healthy adults with normal mobility, and no additional exclusion criteria were applied beyond these conditions.

IMU sensors attached to the right side of the body at four locations were located: the waist (IMU1), thigh (IMU2), calf (IMU3), and heel (IMU4). These placements were selected to capture comprehensive motion data across major lower limb segments during gait. The waist sensor (IMU1) monitors trunk movement and overall body orientation. The thigh (IMU2) and calf (IMU3) sensors were positioned to track the motion of the upper and lower leg segments, which are essential for identifying gait phases such as stance and swing. The heel sensor (IMU4) was placed to detect critical gait events like heel-strike and toe-off with high temporal precision. This sensor configuration enables detailed kinematic analysis and supports the synchronization of segmental limb movements with muscle activity recorded by EMG [27], [28], as illustrated in Fig. 1.

In the Fig. 1, surface EMG sensors were placed on the left leg, specifically on the gastrocnemius (EMG1) and tibialis anterior (EMG2) muscles. These muscles were chosen due to their key roles in gait: the gastrocnemius contributes to plantarflexion during the push-off phase, while the tibialis anterior is responsible for dorsiflexion during the swing phase and helps control foot landing during heel-strike. Monitoring these muscles is essential for analysing muscle activation patterns across the gait cycle [29]. The sensor placement was distinguished by positioning the IMU sensor on the right leg and the EMG sensor on the left side. This configuration was chosen to reduce excessive load on one leg and enhance gait detection's effectiveness [30].

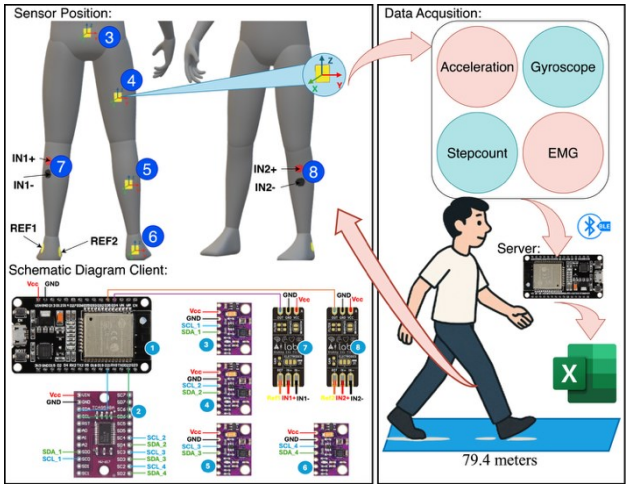


Fig. 1. Overview of the data acquisition system, including IMU and EMG sensor placement on the lower limbs, system schematic diagram, and the process of recording.

The acquisition system employs two ESP32 microcontrollers communicating via Bluetooth Low Energy (BLE), with one configured as a server and the other as a client. The entire system is battery powered. The hardware components used in the data acquisition process are shown in Fig. 1 and consist of: (1) ESP32; (2) TCA9548A multiplexer; (3–6) four IMU sensors; and (7, 8) two EMG sensors. The hardware configuration, comprising an ESP32 microcontroller, an I2C TCA9548A multiplexer. The data is subsequently saved in CSV format using an Excel data stream.

The data collection procedure was conducted in four stages: 10 seconds of IMU sensor calibration, followed by a one-minute rest, walking over 79.4 meters, and another one-minute rest. This sequence was then repeated under fast-walking conditions. Measurements were taken under both slow and fast walking conditions using IMU sensors (to capture acceleration, angular velocity, and step count) and EMG sensors to assess the activity of the gastrocnemius and tibialis anterior muscles. Data acquisition was performed at two different walking speeds: slow and fast walking. These walking conditions were not normalised for speed but rather based on each participant's individual capability and habitual walking pattern.

C. *Gait Analysis and Muscle Function*

Gait analysis is the systematic study of human walking patterns, with significant applications in physiotherapy, rehabilitation, and wearable technology. It involves monitoring and evaluating body movements to understand locomotion mechanics, identify abnormalities, and support therapeutic interventions. The human gait cycle is divided

into two main phases: stance and swing, as illustrated in Fig. 2 [31], [32].

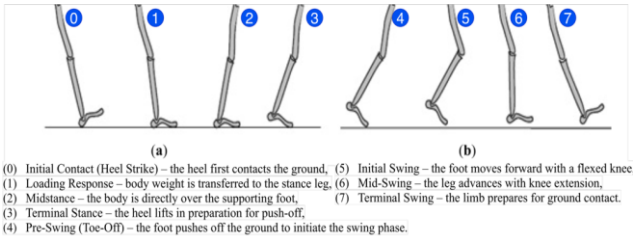


Fig. 2. Phases of gait in a normal gait cycle: (a) Stance Phase; (b) Swing Phase.

The stance phase comprises approximately 60% of the cycle and begins with initial ground contact, ending when the foot lifts off Fig. 2 (a). The swing phase, covering the remaining 40%, starts when the foot leaves the ground and ends upon recontact Fig. 2(b) [31], [32].

Efficient gait relies on coordinated muscle activity. The tibialis anterior facilitates ankle dorsiflexion during the swing phase, aiding foot clearance and preventing tripping. The gastrocnemius contributes to ankle plantarflexion during push-off and helps stabilize the body during landing. These muscles generate the propulsive and stabilizing forces necessary for effective locomotion [32]. According to the definition, one gait cycle consists of two steps, representing the movement from one foot and returning to the same foot [31], [33]. Furthermore, each gait cycle (GC) is divided into eight phases, comprising five phases in the stance phase and three phases in the swing phase, resulting in a total of eight gait phases (GC phase) [31], [33].

D. Inertia Measurement Unit Sensor

IMU sensors are portable devices that integrate accelerometers, gyroscopes, and sometimes magnetometers to measure real-time acceleration, angular velocity, and orientation [34], [35]. This study employs the MPU9250 sensor, which communicates via the I²C (Inter-Integrated Circuit) protocol and is integrated using a TCA9548A multiplexer to expand the number of I²C channels on the controller [36].

IMUs are commonly used in gait analysis to extract key parameters such as acceleration, angular velocity (gyroscope), roll and pitch angles, step count, step duration, and cadence. Acceleration and gyroscopic data capture spatial and temporal movement dynamics, while roll and pitch indicate segment orientation during walking [1].

Step count and step duration provide quantitative metrics on step frequency and timing. Step length and cadence offer insight into gait efficiency and rhythmic patterns [37], [38].

Step count is determined by identifying periodic peaks in vertical or total acceleration signals during walking. Each peak corresponds to a step, and the magnitude of the total acceleration is computed using the vector sum of acceleration in all three axes (2) [17].

E. EMG Sensor

EMG sensors are devices used to record the electrical activity of muscles during the contraction process [39]. In gait analysis, EMG sensors monitor the activity of muscles involved in the phases of the walking cycle, providing vital information about neuromuscular function and motor control patterns. The EMG sensor can be a non-invasive skin surface (surface EMG/sEMG), allowing real-time measurement of muscle activity without disturbing the subject's natural movements [40], [41].

The filter used for the EMG sensor is a Butterworth filter. The Butterworth Band-Pass IIR filter isolates relevant frequencies from EMG signals. This filter belongs to the Infinite Impulse Response (IIR) category and is designed using the Butterworth mathematical function, which is known for its flattest response in the passband [20], [42].

III. RESULTS

This study involved ten male participants, five of whom were classified as obese based on their Body Mass Index (BMI). Table 1 presents detailed participant information.

TABLE I
SUBJECT INFORMATION

Sub	BMI (kg/m²)	Step Count (SW)	Duration (s)	Step Count (FW)	Duration (s)
1	30.1	126	77	113	56
2	45.7	121	67	119	59
3	31.8	132	85	112	57
4	37.8	138	97	118	68
5	39.2	132	95	124	79
6	29.7	128	83	119	62
7	24	118	65	98	47
8	23.4	137	88	128	70
9	20.8	125	75	120	62
10	20.1	129	77	101	58

Note: : Obese; :Normal; SW: Slow Walking; FW: Fast Walking

Table 1 presents data from ten participants, consisting of five individuals classified as obese and five with normal body composition, based on Body Mass Index. On average, obese participants covered a distance of 79.4 m with 129.8 steps during slow walking and 117.2 steps during fast walking. In contrast, normal-weight participants recorded an average of 127.4 steps (slow) and 113.2 steps (fast). For the obese group, walking 79.4 m at a slow pace required 84.2 seconds with 129.8 manually counted steps; the IMU detected 126.6 steps, with an error rate of 2.5%. During fast walking, the average time decreased to 63.8 seconds with 117.2 manually counted steps, while the IMU recorded 113 steps (3.6% error). For the normal-weight group, slow walking required 77.6 seconds with 127.4 manually counted steps; the IMU registered 124 steps (2.7% error). During fast walking, the average time was 59.8 seconds with 113.2 manually counted steps, and the IMU detected 110.8 steps (2.1% error).

Differences in the distribution of acceleration,

gyroscope, and EMG signals were also observed between the two groups. During fast walking, the standard deviation of acceleration was 0.177 g in the obese group and 0.195 g in the normal group; for the gyroscope, the values were 30.305° and 35.897°, respectively. For EMG, the standard deviation of the gastrocnemius signal in the obese group was 726.84 mV and the tibialis anterior 726.92 mV, while in the normal group they were 726.84 mV and 726.94 mV, respectively. However, the EMG differences were relatively small; for example, in the gastrocnemius, the mean signal dispersion for obese participants was 1030.67 mV (slow) vs. 1030.71 mV (fast), compared to 1030.67 mV (slow) vs. 1007.39 mV (fast) in normal participants.

Further evaluation employed the t-test and Mann–Whitney U test to examine the significance of signal differences between the obese and normal groups under slow and fast walking conditions. The test results are summarized in Table 2.

TABLE II
P-VALUES FROM T-TEST AND MANN–WHITNEY U TEST OBESE VS NORMAL GROUPS

Condition	Parameter	T-test (p-value)	Mann–Whitney U (p-value)
Slow Walking	*ax*	< 0.00001	0.00017
	ay	< 0.00001	< 0.00001
	az	0.75473	0.00001
Fast Walking	*ax*	0.00015	0.06763
	ay	< 0.00001	< 0.00001
	az	< 0.00001	< 0.00001
Slow Walking	*gx*	0.02589	< 0.00001
	gy	0.07945	0.60216
	gz	0.50944	0.00002
Fast Walking	*gx*	0.00545	0.63859
	gy	0.82514	0.77202
	gz	0.01062	0.00002
Slow Walking	Gastrocnemius	< 0.00001	< 0.00001
	Tibialis Anterior	< 0.00001	< 0.00001
Fast Walking	Gastrocnemius	< 0.00001	< 0.00001
	Tibialis Anterior	< 0.00001	< 0.00001

Based on the statistical analysis of biomechanical parameters during slow and fast walking, significant differences were identified between the obese and normal groups. Under slow walking conditions, acceleration parameters in the ax and ay axes showed highly significant differences ($p < 0.00001$) in both the t-test and Mann–Whitney U test. In contrast, the *az* axis did not show a meaningful difference in the t-test ($p = 0.75$), but was significant in the non-parametric test ($p = 0.00001$), indicating differences in distribution despite similar mean values. For gyroscope data, only *gx* and *gz* demonstrated partial significance, with *gz* showing a strong difference particularly in the Mann–Whitney U test ($p < 0.00001$), while *gy* did not exhibit a notable difference. EMG data from the gastrocnemius and tibialis anterior muscles revealed highly significant differences between the two groups, with $p < 0.00001$ in both tests.

Under fast walking conditions, all acceleration parameters (*ax*, *ay*, *az*) showed significant differences between the obese and normal groups, although the Mann–Whitney result for *ax* ($p = 0.06763$) was close to the significance threshold. Gyroscope parameters again yielded mixed results, with only *gz* consistently significant, while *gx* and *gy* did not show meaningful differences. Similar to the slow condition, EMG signals from both muscles demonstrated highly significant differences across all statistical tests. Overall, EMG and acceleration signals (particularly *ax* and *ay*) were the most consistent parameters in distinguishing between groups under both slow and fast walking conditions. Gyroscope parameters showed more limited differences, mainly in the *gz* axis, and were not consistent across all conditions.

The HMM analysis was conducted to identify and classify walking phases based on temporal signal patterns. The HMM model employed eight classes corresponding to gait sub-phases, as illustrated in Figure 2. The temporal detection of hidden states is presented in Figure 3.

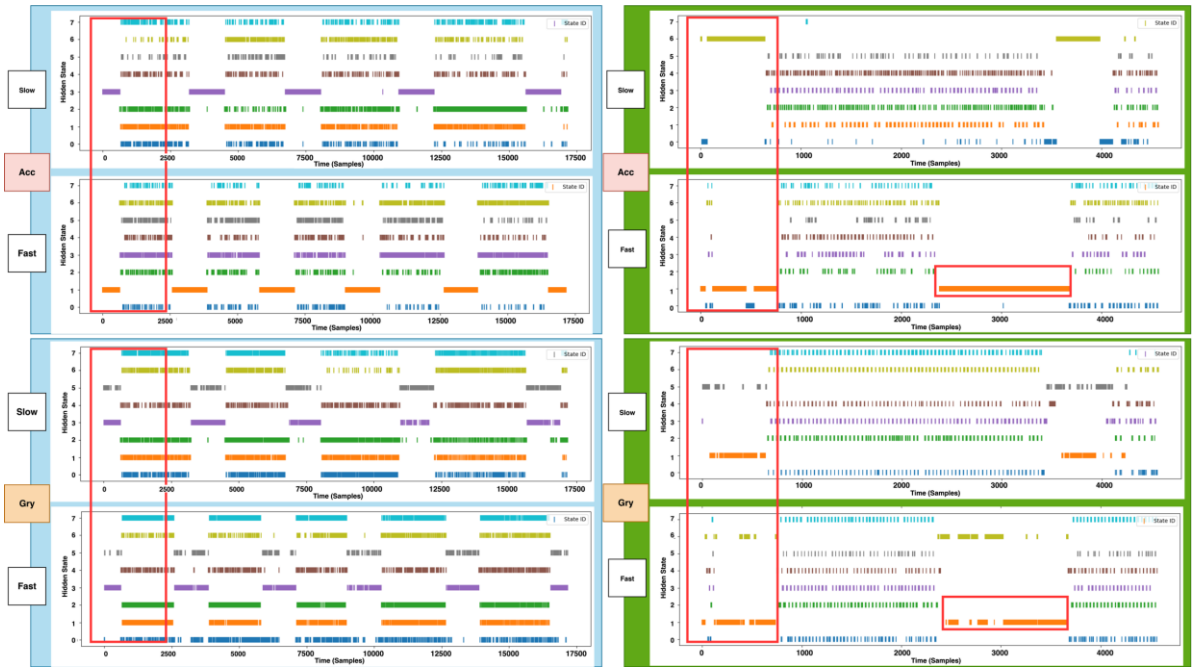


Fig. 3. Comparison of Hidden Markov Model (HMM) detection results based on accelerometer and gyroscope sensors between obese (blue) and normal (green) participants during slow and fast walking activities.

TABLE III
EMISSION DISTRIBUTION PER STATE PARAMETER– SLOW WALKING & FAST WALKING

S	Obese								Normal							
	Acceleration				Gyroscope				Acceleration				Gyroscope			
	Slow Walking		Fast Walking		Slow Walking		Fast Walking		Slow Walking		Fast Walking		Slow Walking		Fast Walking	
	μ_i	σ_i^2	μ_i	σ_i^2	μ_i	σ_i^2	μ_i	σ_i^2	μ_i	σ_i^2	μ_i	σ_i^2	μ_i	σ_i^2	μ_i	σ_i^2
0	-0.025	0.005	-0.034	0.107	-21.452	471.7869	2.4800	39.4285	0.019	0.001	-0.062	0.008	-20.64	249.64	12.096	195.2388
1	-0.002	0.002	-0.002	0.001	3.1414	30.3464	-14.241	321.6102	0.308	0.021	-0.009	<0.001	-0.188	0.0104	-0.240	0.009
2	-0.026	0.002	0.188	0.022	7.2766	91.4820	-5.7877	225.1033	-0.012	0.002	-0.037	0.016	8.124	76.111	6.367	171.133
3	-0.001	0.001	-0.086	0.011	-0.2018	0.0063	-0.2060	0.0242	0.021	0.001	0.374	0.028	7.737	31.339	-29.195	278.003
4	0.2545	0.023	0.302	0.038	14.4652	97.0268	13.9750	170.6377	-0.017	0.006	-0.199	0.007	11.73	0.239	-3.256	155.45
5	0.104	0.049	-0.180	0.016	-0.1932	0.0375	0.0955	0.2217	-0.099	0.017	0.107	0.086	-0.281	27.373	-27.847	163.799
6	-0.137	0.034	0.024	0.003	-6.2795	105.636	7.6617	45.9781	0.005	<0.001	-0.105	0.008	-31.833	330.242	-0.203	0.237
7	0.259	0.017	0.086	0.057	-11.357	71.5289	-8.1789	473.224	0.290	0.022	0.082	0.014	16.051	27.373	-8.161	128.24

In Figure 3, the obese group utilized 17,500 data points (±87.5 seconds), whereas the normal group used only 4,500 data points (±22.5 seconds). This difference arises because obese participants walked for a longer duration (see Table 1). In general, the movement patterns of obese participants appeared simpler and less responsive to changes in walking speed compared to the normal group (Figure 3: green = normal, blue = obese). However, an anomaly was observed in the normal group: at around data point 2500, the acceleration parameter repeatedly detected state 1, although this anomaly was less evident in the gyroscope signal.

To examine the emission and variance of each state in the 8-class HMM model, the results are presented in Table 3. Table 3 shows the emission distribution parameters of the HMM, consisting of the mean (μ) and variance (σ^2) of acceleration and gyroscope signals collected during slow and fast walking activities, for both the obese and normal groups. These data are classified into eight states (S0–S7), representing different stages or patterns in the walking process.

The gyroscope variance (σ^2) in the obese group (state 0: 471.79°) was considerably larger than in the normal group (249.64°) as shown in Table 3, indicating more fluctuating movements in obesity. Furthermore, in the obese group, several states (state 4 and state 7) exhibited relatively high mean (μ) values in acceleration during fast walking (0.30g, 0.08g), whereas in the normal group the μ values were relatively small (<0.1). This suggests that obese individuals generate higher acceleration amplitudes during fast walking, possibly due to biomechanical compensation.

The normal group tended to show higher μ values in several states (state 0: 12.09° vs state 3: 29.19°) compared to the obese group (approximately 2–8). This indicates that during fast walking, normal participants generated more dynamic joint rotations, whereas obese participants showed more limited movement. In contrast, the obese group exhibited relatively higher gyroscope μ values in certain states (state 4: 14.465°), suggesting greater rotational usage.

In the obese group, gyroscope signals during slow walking showed high mean values but decreased as speed increased. Conversely, in the normal group, fast walking was associated with stable variance, indicating more rhythmic steps. Overall, obesity was associated with less efficient gait patterns, characterized by higher acceleration, limited rotation, and greater step variability. In contrast, the normal group demonstrated more stable and consistent gait with better rotational movement, particularly at higher speeds.

In addition, the proportion of detected states is presented in Table 4. Table 4 shows the percentage of detected states in the HMM model based on acceleration (Acc) and gyroscope (Gry) parameters under slow walking (SW) and fast walking (FW) conditions. In obese participants, during slow walking, state 3 dominated the accelerometer parameter with a proportion of 33.4%, followed by states 1 and 2 at 14.7% each. During fast walking, a significant shift occurred, with state 1 becoming the most dominant at 36.6%, while state 3 decreased to 15.4%. Gyroscope data showed a similar tendency, where dominance shifted from state 3 to states 1 and 2 when transitioning from slow to fast walking.

In normal participants, the changes were more pronounced. During fast walking, state 1 became highly dominant in the accelerometer signal at 41.5%, rising sharply from 16.4% during slow walking. State 7, which

was nearly undetected in slow walking (0.3%), increased to 6.6% and 12.9% (in accelerometer and gyroscope, respectively) during fast walking, indicating a more complete and efficient gait cycle. Conversely, the decrease in states 6 and 2 reflected a redistribution of phases as walking speed increased.

TABLE IV
DISTRIBUTION OF HMM MODEL BASED ON ACCELEROMETER (ACC) AND GYROSCOPE (GRY) DURING SLOW WALKING (SW) & FAST WALKING (FW)

Participants	S	Acc-SW (%)	Acc-FW (%)	Gry-SW (%)	Gry-FW (%)
Obese	0	8.1	4.7	9.2	10.6
	1	14.7	36.6	12.8	15.3
	2	14.7	8.9	14.0	18.8
	3	33.4	15.4	17.4	21.6
	4	6.1	7.2	8.3	8.8
	5	4.9	9.2	14.4	9.5
	6	9.4	11.8	11.6	8.2
	7	8.8	6.2	12.3	6.9
Normal	0	9.2	12.5	6.9	10.6
	1	16.4	41.5	17.3	29.8
	2	17.2	6.3	14.5	13.2
	3	13.4	9.8	13.9	10.3
	4	12.9	6.7	10.2	6.2
	5	7.8	6.7	10.4	3.6
	6	22.6	9.7	17.3	13.4
	7	0.3	6.6	9.4	12.9

In addition to the acceleration and gyroscope parameters, the 8-class HMM model was also applied to EMG signals from the gastrocnemius and tibialis anterior muscles under both fast and slow walking conditions in obese participants (blue in Figure 4) and normal participants (green in Figure 4). Figure 4 illustrates the detected states of the HMM model using EMG features, where the root mean square (RMS) was employed. The displayed data sample consists of 420 data points, equivalent to 85 seconds, with a window size of 10.

In Figure 4, obese participants were initially detected in state 4 during slow walking and state 6 during fast walking for the gastrocnemius muscle. For the tibialis anterior, the initial state was detected as state 6 in both slow and fast walking. In contrast, for normal participants, the gastrocnemius muscle showed an initial detection of state 6 during slow walking and state 4 during fast walking. For the tibialis anterior, the initial state was detected as state 6 during slow walking and state 1 during fast walking. Visually, the patterns were dominated by several overlapping states.

In addition, to examine the emission and variance of each state in the 8-class HMM model, the results are presented in Table 5. Table 5 reports the emission distribution parameters of the HMM, consisting of the mean (μ) and variance (σ^2) of the gastrocnemius and tibialis anterior signals, recorded during slow walking and fast walking for both obese and normal groups. The data are classified into eight states (S0–S7), representing distinct phases or patterns within the walking process.

Based on the emission distribution of the Gastrocnemius and Tibialis Anterior during slow and fast walking, marked differences between obese and normal participants are evident in Table 5. In obese group, the gastrocnemius mean values were generally higher in several states, particularly in state 1 (1274.37 for slow walking and 1437.72mV for fast walking), accompanied by large variances (67,235.19mV and 31,954.47mV). This indicates strong muscle activation, reflected in the high variability. Similarly, the tibialis anterior in obese participants exhibited a comparable pattern, with elevated mean values in state 1 (1149.14mV during slow walking and 1267.16mV during fast walking) and large variances (12,130.68mV and 55,044.72mV), suggesting substantial fluctuations in muscle contractions.

Conversely, in normal participants (Table 5), although the mean values of the gastrocnemius and tibialis anterior were also high in certain states (gastrocnemius in states 2 and 3, and tibialis anterior in states 2, 3, and 7), the variances were relatively lower and more stable. For instance, in normal participants, the gastrocnemius during state 1 in fast walking had a mean of 1774.31mV with a variance of 28,846.66, which is smaller compared to the obese group, while the tibialis anterior during state 2 in fast walking had a mean of 1356.15mV with a variance of 16,564.31, still more controlled than in the obese group. This pattern suggests that in the normal group, although muscle activation increases with walking speed, the distribution of muscle activity remains more stable and efficient. Overall, the results in Table 5 confirm that the obese group exhibited greater muscle activation but with higher variability. In contrast, the normal group demonstrated more balanced muscle activation with lower variance.

To examine the distribution of detected states in the 8-state HMM for the gastrocnemius and tibialis anterior muscles, the results are presented in Table 6. Based on Table 6, obese participants showed activation patterns in both the gastrocnemius (GAS) and tibialis anterior (TIB) that were concentrated in a single dominant state, particularly state 1. In the gastrocnemius, state 1 dominated during both slow walking (54.3%) and fast walking (31.2%). A similar trend was observed in the tibialis anterior, especially during fast walking, with a very high proportion (58.1%). Although fast walking exhibited some distribution across other states, such as state 2 (26.9%) and state 6 (20.4%) in the gastrocnemius, the overall activation pattern remained uneven.

In contrast, in normal participants, muscle activation was more evenly distributed across various states as shown in Table 6. In the gastrocnemius during slow walking, state 2 (31.1%), state 3 (14.2%), state 5 (13.7%), state 6 (13.9%), and state 7 (15.6%) all contributed significantly without a single dominant state. During fast walking, activation shifted with an increase in state 1 (34.2%) and state 2 (24.3%), yet the distribution still involved several other states. Tibialis anterior activation was also more balanced, with substantial contributions from states 1, 2, 3, 6, and 7 under both walking conditions.

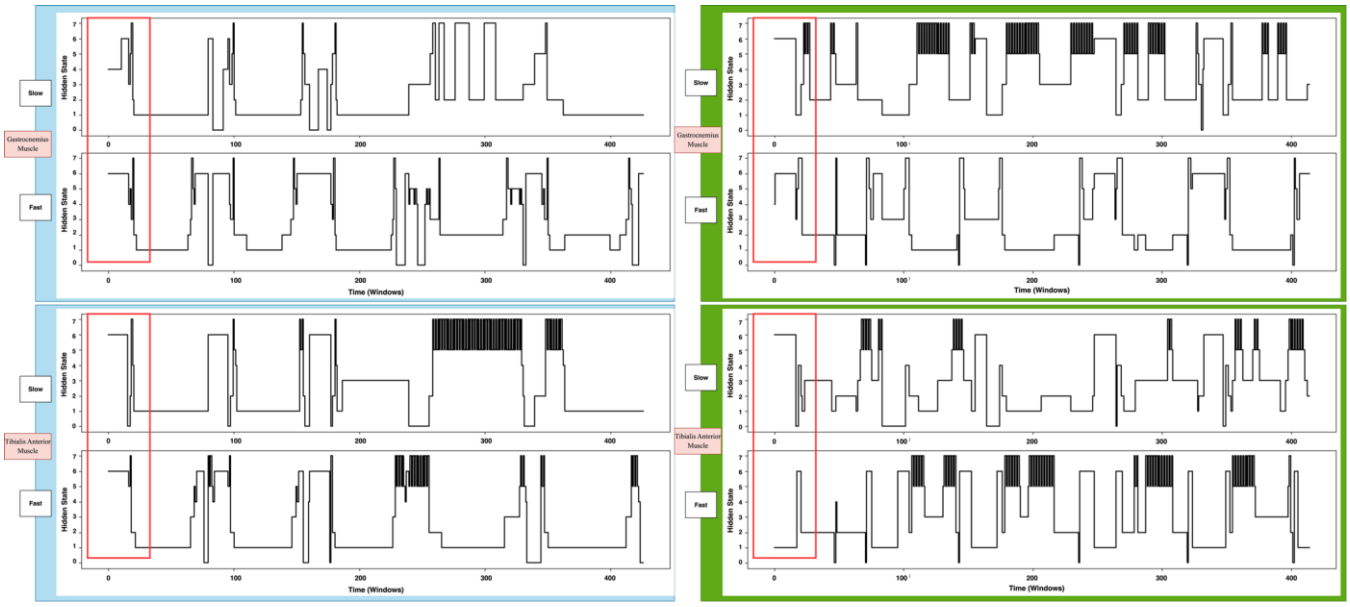


Fig. 4. Comparison of Hidden Markov Model (HMM) detection results based on gastrocnemius and tibialis anterior muscle between obese (blue) and normal (green) participants during slow and fast walking activities.

TABLE V
EMISSION DISTRIBUTION PER STATE PARAMETER– SLOW WALKING & FAST WALKING

S	Obese Participants								Normal Participants							
	Gastrocnemius				Tibialis Anterior				Gastrocnemius				Tibialis Anterior			
	Slow Walking		Fast Walking		Slow Walking		Fast Walking		Slow Walking		Fast Walking		Slow Walking		Fast Walking	
	μ_i	σ_i^2	μ_i	σ_i^2	μ_i	σ_i^2	μ_i	σ_i^2	μ_i	σ_i^2	μ_i	σ_i^2	μ_i	σ_i^2	μ_i	σ_i^2
0	83.74	5.001	171.86	310.63	165.31	1856.36	114.7988	44.59	335.82	34429.07	1018.96	6205.73	242.97	4134.87	976.43	3873.343
1	1274.37	67235.19	1437.72	31954.47	1149.14	12130.68	1267.16	55044.72	335.82	34429.07	1774.31	28846.66	1314.19	3175.59	81.44	1629.08
2	779.99	3025.19	1078.49	10498.12	402.81	11220.74	705.07	24821.13	1653.06	26994.50	1361.09	15718.57	1091.67	14353.75	1356.15	16564.31
3	175.32	2265.08	698.06	14051.05	1698.57	15328.84	499.04	28992.76	1106.27	8507.43	149.39	1751.01	1516.77	7660.03	1965.27	21053.79
4	71.012	27.92	251.13	466.14	891.11	1863.16	125.23	13.25	551.17	0.0100	59.21	0.0100	638.69	24335.35	1034.95	0.0100
5	419.18	7004.17	341.06	2375.22	730.46	7021.65	202.32	2246.25	1336.02	5213.47	321.3929	1725.88	1788.84	24273.59	1696.78	5380.971
6	76.56	664.45	98.29	329.30	75.76	167.007	86.34	74.53	80.39	196.64	57.13	317.71	80.36	194.98	424.35	59527.76
7	619.67	1998.11	676.92	23859.91	722.14	8518.55	231.31	4657.56	1357.43	5434.81	710.95	34869.88	1813.43	23247.68	1678.36	5370.78

The evaluation of the Hidden Markov Model (HMM) for slow walking and fast walking activities with 8 states in obese subjects revealed differences in model quality. The comparison results based on log-likelihood, AIC, and BIC parameters are presented in Table 7.

The evaluation results of the 8-state HMM model in Table 7 demonstrate that the accelerometer (ACC) is the most effective sensor for distinguishing gait patterns in obese individuals compared to normal participants. This is evidenced by the substantially higher log-likelihood values in the obese group, both during slow walking (147,158.66 vs. 39,928.33; an increase of 268.5%) and fast walking (122,401.23 vs. 38,598.62; an increase of 217.1%). This consistency is further reinforced by much lower AIC and BIC values in the obese group (e.g., AIC for slow walking: –293,853.33 vs. –79,392.67 in normal), indicating that the HMM provides a more efficient representation of obese gait patterns when using accelerometer data.

In contrast, the gyroscope (GRY) exhibited poor performance, particularly in the obese group. The log-likelihood values were highly negative and more extreme (–164,654.79 vs. –48,701.41 during slow walking), accompanied by substantially higher AIC and BIC values (329,773.59 vs. 97,866.82). This suggests that gyroscope data in obese individuals are more difficult for the model to predict and less efficient for discriminating gait patterns.

Meanwhile, for the muscle sensors, gastrocnemius (GAS) and tibialis anterior (TIB), the log-likelihood, AIC, and BIC values were relatively close between obese and normal participants (e.g., GAS slow walking: –2,677.35 vs. –2,542.59; TIB slow walking: –2,546.59 vs. –2,492.17). This indicates that muscle activation patterns

are more stable and consistent across both groups and are not highly sensitive in differentiating obesity from normal conditions.

Overall, these findings highlight that the accelerometer is the most optimal sensor for detecting gait differences between obese and normal groups, while the gyroscope is less efficient, and muscle sensors primarily reflect the stability of muscle activation rather than differences in body condition.

TABLE VI
DISTRIBUTION OF HMM MODEL BASED ON GASTROCNEMIUS (GAS) AND TIBIALIS ANTERIOR (TIB) DURING SLOW WALKING (SW) AND FAST WALKING (FW)

Participants	S	Gas-SW (%)	Gas-FW (%)	Tib-SW (%)	Tib-FW (%)
Obese	0	4.2%	5.6%	7.7%	5.2%
	1	54.3%	31.2%	41.2%	58.1%
	2	14.7%	26.9%	4.5%	4.9%
	3	7.9%	5.2%	12.4%	5.6%
	4	5.2%	3.5%	1.2%	1.6%
	5	3.7%	4.9%	10.3%	5.8%
	6	2.6%	20.4%	11.5%	13.1%
	7	7.3%	2.3%	11.2%	5.6%
Normal	0	0.2%	1.5%	7.9%	1.5%
	1	10.8%	34.2%	20.0%	26.5%
	2	31.1%	24.3%	14.7%	24.8%
	3	14.2%	13.7%	28.7%	10.8%
	4	0.2%	0.2%	2.9%	0.2%
	5	13.7%	2.6%	6.3%	11.3%
	6	13.9%	17.4%	13.9%	13.0%
	7	15.6%	6.0%	5.5%	11.8%

IV. DISCUSSIONS

Based on the evaluation of the wearable system, the findings were consistent with previous studies, showing that in general, obese individuals exhibit shorter step length, slower walking speed, wider step width, and longer double-support time compared to individuals with normal body weight [10], [11]. The wearable device results indicated 129.8 steps during slow walking and 117.2 steps during fast walking for obese participants, compared to 127.4 steps during slow walking and 113.2 steps during fast walking for normal-weight participants. However, the most accurate step detection was achieved using an IMU sensor placed on the heel, which yielded an accuracy of approximately 95% in step detection and demonstrated reliable performance in identifying heel-strike and toe-off events [43], [44]. In addition, the shank-mounted sensor provided the closest results to the manually counted steps, with an average error rate of 33.13%. These findings highlight that sensor placement on the lower extremities, particularly on the foot or shank, offers promising accuracy in step detection [45]. Such evidence may serve as a foundation for the development of personalized rehabilitation strategies by identifying phase-specific deficits, thereby enabling more targeted interventions based on the accuracy of sensor placement.

TABLE VII
HMM 8-STATE MODEL EVALUATION METRICS FOR ACCELEROMETER (ACC), GYROSCOPE (GRY), GASTROCNEMIUS (GAS), AND TIBIALIS ANTERIOR (TIB)

Metrics	Information	
Log-likelihood	Obese:	
	Acc - Slow Walking	: 147158.66
	Acc - Fast Walking	: 122401.23
	Gry - Slow Walking	:-164654.79
	Gry - Fast Walking	: -188155.67
	Gas - Slow Walking	: -2677.35
	Gas - Fast Walking	: -2574.15
	Tib - Slow Walking	: -2546.59
	Tib - Fast Walking	: -2661.54
	Normal:	
	Acc - Slow Walking	: 39928.33
	Acc - Fast Walking	: 38598.62
	Gry - Slow Walking	: -48701.41
	Gry - Fast Walking	: -42452.68,
	Gas - Slow Walking	: -2542.59
	Gas - Fast Walking	: -2547.19
	Tib - Slow Walking	: -2492.17
	Tib - Fast Walking:	: -2569.62
AIC	Obese:	
	Acc - Slow Walking	: -293853.33
	Acc - Fast Walking	: -244338.47
	Gry - Slow Walking	: 329773.59
	Gry - Fast Walking	: 376775.34
	Gas - Slow Walking	: 5530.71
	Gas - Fast Walking	: 5324.30
	Tib - Slow Walking	: 5269.17
	Tib - Fast Walking	: 5499.08
	Normal:	
	Acc - Slow Walking	: -79392.67
	Acc - Fast Walking	: -76733.24
	Gry - Slow Walking	: 97866.82
	Gry - Fast Walking	: 85369.37
	Gas - Slow Walking	: 5261.18
	Gas - Fast Walking	: 5270.37
	Tib - Slow Walking	: 5160.35
	Tib - Fast Walking	: 5315.24
BIC	Obese:	
	Acc - Slow Walking	: -292055.16
	Acc - Fast Walking	: -242540.29
	Gry - Slow Walking	: 331571.76
	Gry - Fast Walking	: 378573.51
	Gas - Slow Walking	: 5887.71
	Gas - Fast Walking	: 5681.30
	Tib - Slow Walking	: 5626.17
	Tib - Fast Walking	: 5856.08
	Normal:	
	Acc - Slow Walking	: -77901.64
	Acc - Fast Walking	: -75242.21
	Gry - Slow Walking	: 99357.85
	Gry - Fast Walking	: 86860.39
	Gas - Slow Walking	: 5615.67
	Gas - Fast Walking	: 5624.86
	Tib - Slow Walking	: 5514.83
	Tib - Fast Walking	: 5669.73

Based on the statistical analysis, EMG signals and acceleration (particularly ax and ay) were the most consistent parameters in distinguishing between groups, both at slow and fast walking speeds. However, gait

differences may be influenced by multiple factors, including musculoskeletal disorders, neurological impairments, biomechanical alterations due to obesity, compensatory mechanisms related to pain, joint deformities, as well as deficits in motor control or proprioception [46]. Nevertheless, other findings have reported that individuals with obesity exhibit distinctive biomechanical adaptations even in the absence of pain or injury, suggesting that these adaptations cannot be fully explained by pathological factors alone [8], [9].

Furthermore, while HMM models are often considered effective with 4–6 states [23], the findings of this study indicate that using 8 states provides a more comprehensive description of gait phase differences, consistent with the number of gait sub-phases. However, the results still could not clearly distinguish the initial phase as expected. This is evident in the temporal sequence, where the first detected state was not state 0 (initial contact). For IMU sensor parameters, the obese group was predominantly represented by state 3, whereas the normal group was dominated by state 1. In contrast, for EMG parameters, both obese and normal participants were primarily dominated by state 1, based on the percentage distribution of detected states in the HMM model.

The evaluation of the HMM with 8 states revealed that accelerometer parameters were the most informative for distinguishing gait patterns between obese and normal groups, whereas the gyroscope demonstrated poorer modeling performance in the obese group, and muscle signals tended not to show prominent differences between groups. These findings are consistent with previous research, which reported that accelerometers exhibit strong capabilities in extracting features associated with BMI conditions [47]. In contrast, EMG parameters from the gastrocnemius and tibialis anterior muscles did not show significant differences with respect to body mass variation [48]. However, this outcome may also be influenced by other factors, such as subcutaneous fat or skin layers [49]. Furthermore, differences in sensor placement between EMG and IMU may have contributed to potential asymmetry in gait patterns.

Although the results revealed significant differences between the obese and normal groups, this study did not include specific screening for conditions such as osteoarthritis, lower limb injuries, balance disorders, or chronic pain. These factors may also influence gait characteristics and therefore could have contributed to the variations observed in the results. Future studies should incorporate comprehensive screening protocols to control for these potential confounding variables. The findings of this study apply to the current study population; however, further verification is required to determine the extent to which these findings can be generalized to broader and more diverse populations.

V. CONCLUSION

This study demonstrated that obese participants took an average of 129.8 steps in 84.2 seconds during slow walking and 117.2 steps in 63.8 seconds during fast walking, whereas normal participants recorded an average of 127.4 steps in 77.6 seconds (slow) and 113.2 steps in 59.8 seconds (fast). Statistical analysis revealed significant differences in acceleration along the ax and ay axes ($p < 0.00001$) during both slow and fast walking, as well as in the EMG signals of the gastrocnemius and tibialis anterior muscles ($p < 0.00001$). The variance of the gyroscope signal in the obese group (state 0: 471.8) was higher than in the normal group (249.6), indicating greater movement fluctuations. In the 8-state HMM distribution, the gait pattern of obese participants was dominated by a single state, for example, gastrocnemius state 1 accounted for 54.3% (slow) and 31.2% (fast), and tibialis anterior state 1 reached 58.1% (fast). In contrast, normal participants exhibited a more evenly distributed pattern (e.g., gastrocnemius state 2: 31.1% slow and 24.3% fast). HMM model evaluation identified the accelerometer as the most informative sensor, yielding the highest log-likelihood values (obese slow walking: 147,158.66 vs. normal slow walking: 39,928.33), whereas the gyroscope produced highly negative log-likelihoods in obesity (e.g., –188,155.67 during fast walking), indicating less accurate prediction. Overall, obesity results in a gait pattern that is less efficient, more fluctuating, and less adaptive to increased walking speed, whereas normal participants exhibit a more stable and efficient pattern. The integration of multimodal sensors with HMM proved effective in distinguishing between the two groups, with the accelerometer serving as the key parameter.

Although the findings demonstrate significant differences between obese and normal groups, this study did not implement specific screening for comorbid conditions or other factors that may potentially influence gait characteristics. Future research should incorporate comprehensive screening protocols to control for these potential confounders, and additional validation is required to establish the extent to which the present results can be generalized to broader and more heterogeneous populations. Moreover, the absence of gait speed normalization in the current study may have introduced confounding effects into the analysis. Accordingly, subsequent studies should apply standardized speed normalization procedures to enhance the robustness and comparability of gait data across groups.

ACKNOWLEDGMENT

The authors gratefully acknowledge Telkom University for its continuous academic support and the provision of research facilities throughout this study. They also sincerely thank the Telkom University Research and Community Service Centre (PPM) for the financial

support and facilitation. Furthermore, the authors are deeply thankful to Dr. Husneni Mukhtar and all participants who generously contributed to the data collection and system development process.

REFERENCES

[1] G. Prisco *et al.*, "Validity of Wearable Inertial Sensors for Gait Analysis: A Systematic Review," Jan. 01, 2025, *Multidisciplinary Digital Publishing Institute (MDPI)*. doi: 10.3390/diagnostics15010036.

[2] M. C. Schall, H. Chen, and L. Cavuoto, "Wearable inertial sensors for objective kinematic assessments: A brief overview," *J Occup Environ Hyg*, vol. 19, no. 9, pp. 501–508, 2022, doi: 10.1080/15459624.2022.2100407.

[3] H. Prasanth *et al.*, "Wearable sensor-based real-time gait detection: A systematic review," Apr. 02, 2021, *MDPI AG*. doi: 10.3390/s21082727.

[4] S. Scataglini, L. Dellaert, L. Meeuwssen, E. Staeljanssens, and S. Truijen, "The difference in gait pattern between adults with obesity and adults with a normal weight, assessed with 3D-4D gait analysis devices: a systematic review and meta-analysis," 2025.

[5] A. K. Fitch and H. E. Bays, "Obesity definition, diagnosis, bias, standard operating procedures (SOPs), and telehealth: An Obesity Medicine Association (OMA) Clinical Practice Statement (CPS) 2022," *Obesity Pillars*, vol. 1, Mar. 2022, doi: 10.1016/j.obpill.2021.100004.

[6] N. H. Phelps *et al.*, "Worldwide trends in underweight and obesity from 1990 to 2022: a pooled analysis of 3663 population-representative studies with 222 million children, adolescents, and adults," *The Lancet*, vol. 403, no. 10431, pp. 1027–1050, Mar. 2024, doi: 10.1016/S0140-6736(23)02750-2.

[7] N. Malesevic, I. Svensson, G. Hägglund, and C. Antfolk, "An Integrated Approach for Real-Time Monitoring of Knee Dynamics with IMUs and Multichannel EMG," *Sensors*, vol. 23, no. 21, p. 8955, Nov. 2023, doi: 10.3390/s23218955.

[8] A. Patoz, A. F. Menéndez, and D. Malatesta, "The effect of severe obesity on three-dimensional ground reaction force signals during walking," *Clinical Biomechanics*, vol. 107, Jul. 2023, doi: 10.1016/j.clinbiomech.2023.106042.

[9] J. S. Li, T. Y. Tsai, M. M. Clancy, G. Li, C. L. Lewis, and D. T. Felson, "Weight loss changed gait kinematics in individuals with obesity and knee pain," *Gait Posture*, vol. 68, pp. 461–465, Feb. 2019, doi: 10.1016/j.gaitpost.2018.12.031.

[10] J. Rekant, S. Rothenberger, and A. Chambers, "Obesity-Specific Considerations for Assessing Gait with Inertial Measurement Unit-Based vs. Optokinetic Motion Capture," *Sensors*, vol. 24, no. 4, Feb. 2024, doi: 10.3390/s24041232.

[11] V. Agostini, L. Gastaldi, V. Rosso, M. Knaflitz, and S. Tadano, "A wearable magneto-inertial system for gait analysis (H-gait): Validation on normalweight and overweight/obese young healthy adults," *Sensors (Switzerland)*, vol. 17, no. 10, Oct. 2017, doi: 10.3390/s17102406.

[12] S. Haufe, I. U. Isaias, F. Pellegrini, and C. Palmisano, "Gait Event Prediction Using Surface Electromyography in Parkinsonian Patients," *Bioengineering*, vol. 10, no. 2, Feb. 2023, doi: 10.3390/bioengineering10020212.

[13] W. Maktouf *et al.*, "The influence of obesity and fat distribution on ankle muscle coactivation during gait," *PLoS One*, vol. 19, no. 3 March, Mar. 2024, doi: 10.1371/journal.pone.0294692.

[14] A. Makino *et al.*, "Ground reaction force and electromyograms of lower limb muscles during fast walking," *Front Sports Act Living*, vol. 4, 2022, doi: 10.3389/fspor.2022.1055302.

[15] F. Pennoni, F. Bartolucci, and S. Pandofi, "Variable Selection for Hidden Markov Models with Continuous Variables and Missing Data," *J Classif*, Nov. 2024, doi: 10.1007/s00357-023-09457-9.

[16] J. Van Den Broeck, S. A. Cunningham, R. Eeckels, and K. Herbst, "Data cleaning: Detecting, diagnosing, and editing data abnormalities," 2005. doi: 10.1371/journal.pmed.0020267.

[17] J. S. Sheu, W. C. Jheng, and C. H. Hsiao, "Implementation of a three-dimensional pedometer automatic accumulating walking or jogging motions in arbitrary placement," *Int J Antennas Propag*, vol. 2014, 2014, doi: 10.1155/2014/372814.

[18] X. Li, J. Liu, Y. Huang, D. Wang, and Y. Miao, "Human Motion Pattern Recognition and Feature Extraction: An Approach Using Multi-Information Fusion," *Micromachines (Basel)*, vol. 13, no. 8, Aug. 2022, doi: 10.3390/mi13081205.

[19] P. Podder, M. M. Hasan, M. R. Islam, and M. Sayeed, "Design and Implementation of Butterworth, Chebyshev-I and Elliptic Filter for Speech Signal Analysis," 2014.

[20] M. Shouran and E. Elgamli, "Design and Implementation of Butterworth Filter," *Int J Innov Res Sci Eng Technol*, 2020, [Online]. Available: www.ijirset.com

[21] A. Ghasemi and S. Zahediasl, "Normality tests for statistical analysis: A guide for non-statisticians," *Int J Endocrinol Metab*, vol. 10, no. 2, pp. 486–489, 2012, doi: 10.5812/ijem.3505.

[22] L. R. Rabiner, "A Tutorial on Hidden Markov Models and Selected Applications in Speech Recognition," 1989.

[23] A. Mannini and A. M. Sabatini, "Gait phase detection and discrimination between walking-jogging activities using hidden Markov models applied to foot motion data from a gyroscope," *Gait Posture*, vol. 36, no. 4, pp. 657–661, Sep. 2012, doi: 10.1016/j.gaitpost.2012.06.017.

[24] L. Liu *et al.*, "Ambulatory human gait phase detection using wearable inertial sensors and Hidden Markov model," *Sensors (Switzerland)*, vol. 21, no. 4, pp. 1–24, Feb. 2021, doi: 10.3390/s21041347.

[25] T. Bacri, G. D. Berentsen, J. Bulla, and B. Støve, "Computational issues in parameter estimation for hidden Markov models with template model builder," *J Stat Comput Simul*, vol. 93, no. 18, pp. 3421–3457, 2023, doi: 10.1080/00949655.2023.2226788.

[26] F. J. Ochando, A. Cantero, J. I. Guerrero, and C. León, "Data Acquisition for Condition Monitoring in Tactical Vehicles: On-Board Computer Development," *Sensors*, vol. 23, no. 12, Jun. 2023, doi: 10.3390/s23125645.

[27] S. Lin *et al.*, "A Review of Gait Analysis Using Gyroscopes and Inertial Measurement Units," Jun. 01, 2025, *Multidisciplinary Digital Publishing Institute (MDPI)*. doi: 10.3390/s25113481.

[28] L. K. Ramasamy, F. Khan, M. Shah, B. V. V. S. Prasad, C. Iwendi, and C. Biamba, "Secure Smart Wearable Computing through Artificial Intelligence-Enabled Internet of Things and Cyber-Physical Systems for Health Monitoring," *Sensors*, vol. 22, no. 3, Feb. 2022, doi: 10.3390/s22031076.

[29] M. Seynaeve, D. Mantini, and T. T. de Beukelaar, "Electrophysiological Approaches to Understanding Brain–Muscle Interactions During Gait: A Systematic Review," May 01, 2025, *Multidisciplinary Digital Publishing Institute (MDPI)*. doi: 10.3390/bioengineering12050471.

[30] M. Goršič, B. Dai, and D. Novak, "Load position and weight classification during carrying gait using wearable inertial and electromyographic sensors," *Sensors (Switzerland)*, vol. 20, no. 17, pp. 1–14, Sep. 2020, doi: 10.3390/s20174963.

[31] W. Tao, T. Liu, R. Zheng, and H. Feng, "Gait analysis using wearable sensors," Feb. 2012. doi: 10.3390/s120202255.

[32] H. S. Lee, J. H. Lee, and H. S. Kim, "Activities of ankle muscles during gait analyzed by simulation using the human musculoskeletal model," *J Exerc Rehabil*, vol. 15, no. 2, pp. 229–234, Apr. 2019, doi: 10.12965/jer.1938054.027.

[33] A. Kharb, V. Saini, Y. K. Jain, and S. Dhiman, "A review of gait cycle and its parameters," 2011. [Online]. Available: www.IJCEM.orgIJCEMwww.ijcem.org

[34] G. G. Samatas and T. P. Pachidis, "Inertial Measurement Units (IMUs) in Mobile Robots over the Last Five Years: A Review," Feb. 01, 2022, *MDPI*. doi: 10.3390/designs6010017.

[35] Z. Song, Z. Cao, Z. Li, J. Wang, and Y. Liu, "Inertial Motion Tracking on Mobile and Wearable Devices: Recent Advancements and Challenges," 2021.

[36] S. Komarizadehasl, B. Mobaraki, H. Ma, J. A. Lozano-Galant, and J. Turmo, "Development of a low-cost system for the accurate measurement of structural vibrations," *Sensors*, vol. 21, no. 18, Sep. 2021, doi: 10.3390/s21186191.

[37] A. M. Sabatini, "Estimating three-dimensional orientation of human body parts by inertial/magnetic sensing," Feb. 2011. doi: 10.3390/s110201489.

[38] A. J. L. H. R. V. Sebastian O.H. Madgwick, *Estimation of IMU and MARG orientation using a gradient descent algorithm*. IEEE, 2011.

[39] K. Daunoraviciene, J. Ziziene, J. Pauk, G. Juskeniene, and J. Raistenskis, "EMG based analysis of gait symmetry in healthy children," *Sensors*, vol. 21, no. 17, Sep. 2021, doi: 10.3390/s21175983.

[40] V. Agostini, M. Ghislieri, S. Rosati, G. Balestra, and M. Knaflitz, "Surface Electromyography Applied to Gait Analysis: How to Improve Its Impact in Clinics?," *Front Neurol*, vol. 11, Sep. 2020, doi: 10.3389/fneur.2020.00994.

[41] S. Negi, S. Sharma, and N. Sharma, "FSR and IMU sensors-based human gait phase detection and its correlation with EMG signal for different terrain walk," *Sensor Review*, vol. 41, no. 3, pp. 235–245, 2020, doi: 10.1108/SR-10-2020-0249.

[42] WHO, *Obesity : preventing and managing the global epidemic : report of a WHO consultation*. World Health Organization, 2000.

[43] G. Santicchi *et al.*, "Validation of Step Detection and Distance Calculation Algorithms for Soccer Performance Monitoring," *Sensors*, vol. 24, no. 11, Jun. 2024, doi: 10.3390/s24113343.

[44] G. Pacini Panebianco, M. C. Bisi, R. Stagni, and S. Fantozzi, "Analysis of the performance of 17 algorithms from a systematic review: Influence of sensor position, analysed variable and computational approach in gait timing estimation from IMU measurements," *Gait Posture*, vol. 66, pp. 76–82, Oct. 2018, doi: 10.1016/j.gaitpost.2018.08.025.

[45] W. Niswander and K. Kontson, "Evaluating the impact of imu sensor location and walking task on accuracy of gait event detection algorithms," *Sensors*, vol. 21, no. 12, Jun. 2021, doi: 10.3390/s21123989.

[46] J. Runhaar, B. W. Koes, S. Clockaerts, and S. M. A. Bierma-Zeinstra, "A systematic review on changed biomechanics of lower extremities in obese individuals: A possible role in development of osteoarthritis," *Obesity Reviews*, vol. 12, no. 12, pp. 1071–1082, Dec. 2011, doi: 10.1111/j.1467-789X.2011.00916.x.

[47] L. Koinis, M. Maharaj, P. Natarajan, R. D. Fonseka, V. Fernando, and R. J. Mobbs, "Exploring the Influence of BMI on Gait Metrics: A Comprehensive Analysis of Spatiotemporal Parameters and Stability Indicators," *Sensors*, vol. 24, no. 19, Oct. 2024, doi: 10.3390/s24196484.

[48] W. Maktouf *et al.*, "The influence of obesity and fat distribution on ankle muscle coactivation during gait," *PLoS One*, vol. 19, no. 3 March, Mar. 2024, doi: 10.1371/journal.pone.0294692.

[49] T. A. Kuiken, M. M. Lowery, and N. S. Stoykov, "The effect of subcutaneous fat on myoelectric signal amplitude and cross-talk," *Prosthet Orthot Int*, vol. 27, no. 1, pp. 48–54, 2003, doi: 10.3109/03093640309167976.



Suto Setiyadi obtained his Bachelor of Engineering (S.T.) degree from Telkom University in 2021 and subsequently received his Master of Engineering (M.T.) degree from the same university in 2023. His research activities began at the Microprocessor and Interface Laboratory and the Electronics Laboratory. After completing his undergraduate studies, he worked as a research assistant at Bandung Techno Park. Following his master's graduation, he continued his academic career as a lecturer and researcher at the School of Electrical Engineering, Telkom University, Indonesia. He authorises the textbook *Sensor and Actuator with the Cases of Implementation* (Tel-U Press, 2022). His primary research interests include biomedical applications of computer vision and embedded systems.
(email: sutosetiyadisod@telkomuniversity.ac.id)



Muhammad Ridho Rosa received his B.Sc. degree in Physics Engineering from the Bandung Institute of Technology, Indonesia, in 2014, and his M.Sc. degree in Embedded Systems with a specialization in Systems and Control from Delft University of Technology, Netherlands, in 2018. He is currently a lecturer at the School of Electrical Engineering, Telkom University, Indonesia, and is pursuing his Ph.D. degree at the University of Groningen, Netherlands. His research interests include adaptive control and multi-agent control with applications in robotics.
(email: mridhorosa@telkomuniversity.ac.id)



Nigel Bryan Tang is an undergraduate student in the Electrical Engineering program at Telkom University, Indonesia. He is currently active as a laboratory assistant in the Microprocessor and Interface Laboratory, where he is involved in practical sessions, technical assistance, and the development of microcontroller-based and embedded system projects. His interests include hardware programming, embedded systems, and sensor integration for Internet of Things (IoT) and automation applications.
(email: nigelbryan@student.telkomuniversity.ac.id)



Muhammad Sabiq Al Muttaqin is an undergraduate student in the Electrical Engineering program at Telkom University, Indonesia. He is currently active as a laboratory assistant in the Microprocessor and Interface Laboratory, where he assists in practical sessions and provides technical support. His research interests focus on Printed Circuit Board (PCB) design. He is actively involved in projects related to the design of efficient and environmentally friendly electronic systems, with a particular interest in hardware integration for smart energy systems.
(email: msabiqobic@student.telkomuniversity.ac.id)



Muhammad Rafi Haykal Gumelar is an undergraduate student in the Electrical Engineering program at Telkom University, Indonesia. He is currently a laboratory assistant in the Microprocessor and Interface Laboratory, where he is involved in hands-on laboratory sessions and provides technical assistance. His research interests are on embedded systems and hardware programming, particularly in developing microcontroller-based applications and sensor integration. He actively participates in various academic and technical projects related to automation, the Internet of Things (IoT), and hardware-based control systems.
(email: rafihaykal@student.telkomuniversity.ac.id).